Effect of Nodule Count and Cooling Rate on As-Cast Matrix of a Cu-Mo Spheroidal Graphite

R. Salazar F., M. Herrera-Trejo, M. Castro, J. Méndez N., J. Torres T., and M. Méndez N.

(Submitted 8 July 1998; in revised form 26 January 1999)

The transformation of austenite to ferrite and graphite or to pearlite in spheroidal graphite cast iron depends on a number of factors, among which are the nodule count and the cooling rate. In this study, the pearlite fraction decreased as the nodule count increased for a given cooling rate. Furthermore, as the cooling rate increased, the fraction of pearlite increased. Both effects were more sensitive at low nodule count. The effects of altering these parameters on the relative amount of pearlite and ferrite in the matrix of a copper-molybdenum (Cu-Mo) spheroidal graphite cast iron were addressed using heats carried out in an induction furnace, and the melts were treated with magnesium ferrosilicon in a ladle. To vary the nodule count, the melts were inoculated with two different amounts of ferrosilicon. Pouring was performed into sand molds of cylindrical cavities with different section size in order to achieve various cooling rates. Both the nodule count and the cooling rate affected the relative amount of ferrite and pearlite in the matrix.

Keywords cooling rate, inoculation, nodule count, spheroidal graphite

1. Introduction

Austempering is a relatively new treatment applied to specific spheroidal cast irons. The thermal cycle involves heating up to complete austenitization and then controlled cooling to avoid any transformation until the temperature of the isothermal treatment is achieved (Ref 1). In order to treat large sections successfully, the chemical composition is modified with element additions that increase the hardenability of the alloy. (Some of the element additions also affect the isothermal treatment.) Among the elements more widely used are nickel, copper, and molybdenum (Ref 2). It is also essential to control the austenitization stage because it influences the isothermal treatment and therefore the final properties.

The austenitization consists of the transformation of the as-cast microstructure matrix to austenite and its complete carbon saturation. The austenitization stage obviously depends on the as-cast microstructure matrix, and it also depends on the temperature and time of process duration. It has been observed that the ferritic matrix takes a much longer austenitization time than the pearlitic matrix requires at a given temperature. Also, at a low nodule count the carbon saturation of the matrix takes more time than at a high nodule count (Ref 2, 3). Although an austenitization time longer than necessary does not modify the mechanical properties, it increases the manufacturing costs, hence underlying the importance of the control of the as-cast microstructure.

R. Salazar F., Instituto Tecnológico de Saltillo, Blvd. V. Carranza 2400, Apdo. Postal No. 600, 25280 Saltillo, Coah., Mexico; and **M. Herrera-Trejo, M. Castro, J. Méndez N., J. Torres T.,** and **M. Méndez N.,** Centro de Investigación y de Estudios, Avanzados del IPN Unidad Saltillo, Carr. Saltillo-Mty. Km. 13, Apdo. Postal No. 663, 25000 Saltillo, Coah., Mexico. Contact e-mail: mherrera@saltillo.cinvestav.mx.

The as-cast microstructure is governed by the solidification process and also by the subsequent solid state transformation (eutectoid reaction). The inoculation practice and the cooling rate control the nodule count, while the matrix microstructure depends on the conditions under which the eutectoid reaction occurs (Ref 4-7). Among the variables that influence the mechanism of the eutectoid reaction are the chemical composition, the cooling rate through the eutectoid temperature range, and the nodule count (Ref 8-14).

It is clear that a number of parameters influence the as-cast microstructure matrix of spheroidal graphite cast iron and that a control of the solidification process is desirable for optimizing the austenitization stage. It is noteworthy that quantitative studies on the eutectoid reaction in alloyed spheroidal graphite cast iron are not abundant in the literature. The present work to study the effect of nodule count and cooling rate on the as-cast microstructure matrix of such iron was undertaken as part of a series of studies aimed at optimizing the austenitization stage

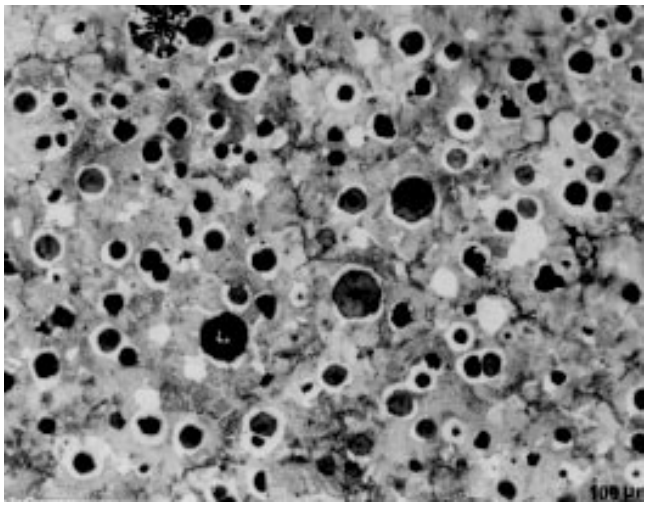

Fig. 1 Typical microstructure. Graphite nodules surrounded by a ferrite shell and pearlite phase

of a thermal cycle of austempering for a Cu-Mo spheroidal graphite iron.

2. Experimental

Seven melts using scrap of ductile cast iron and steel were prepared in a 80 kg capacity induction furnace. After adjusting the chemical composition, sampling of the melt was carried out for posterior chemical analysis by emission spectroscopy technique for all elements except the carbon and sulfur, which were determined by fusion technique. The melt was subsequently transferred into a tundish cover reactor where the melt was treated with magnesium ferrosilicon. The melt was then poured into a ladle as a stage prior to the casting operation. During the transfer operation to the ladle, inoculation was performed as follows: three melts were added with 0.32 wt%, three others were added with 0.64 wt%, and one melt was not inoculated.

Casting was performed into sand molds of cylindrical cavities of 27 mm height and of various diameters (15.5, 22.5, 30, and 53.5 mm) in order to achieve various cooling rates. Some molds were instrumented with Chromel-Alumel thermocouples linked to a computer in order to register the cooling curve. The thermocouples were positioned on the vertical axis at midheight of the mold. After solidification, the cylinders were transversely sectioned at the location of the thermocouple.

After metallographic preparation, the sections were observed under optical microscope for a preliminary analysis. Measurements of nodule count, defined as the number of nodules per squared millimeter, and percentages of ferrite and pearlite were made using an image analyzer. Table 1 shows the heat identification, the associated inoculation percentage, and the chemical composition of the main elements. For all heats, aluminum and phosphorus contents were lower than 0.02%, and nickel and chromium contents were lower than 0.04%.

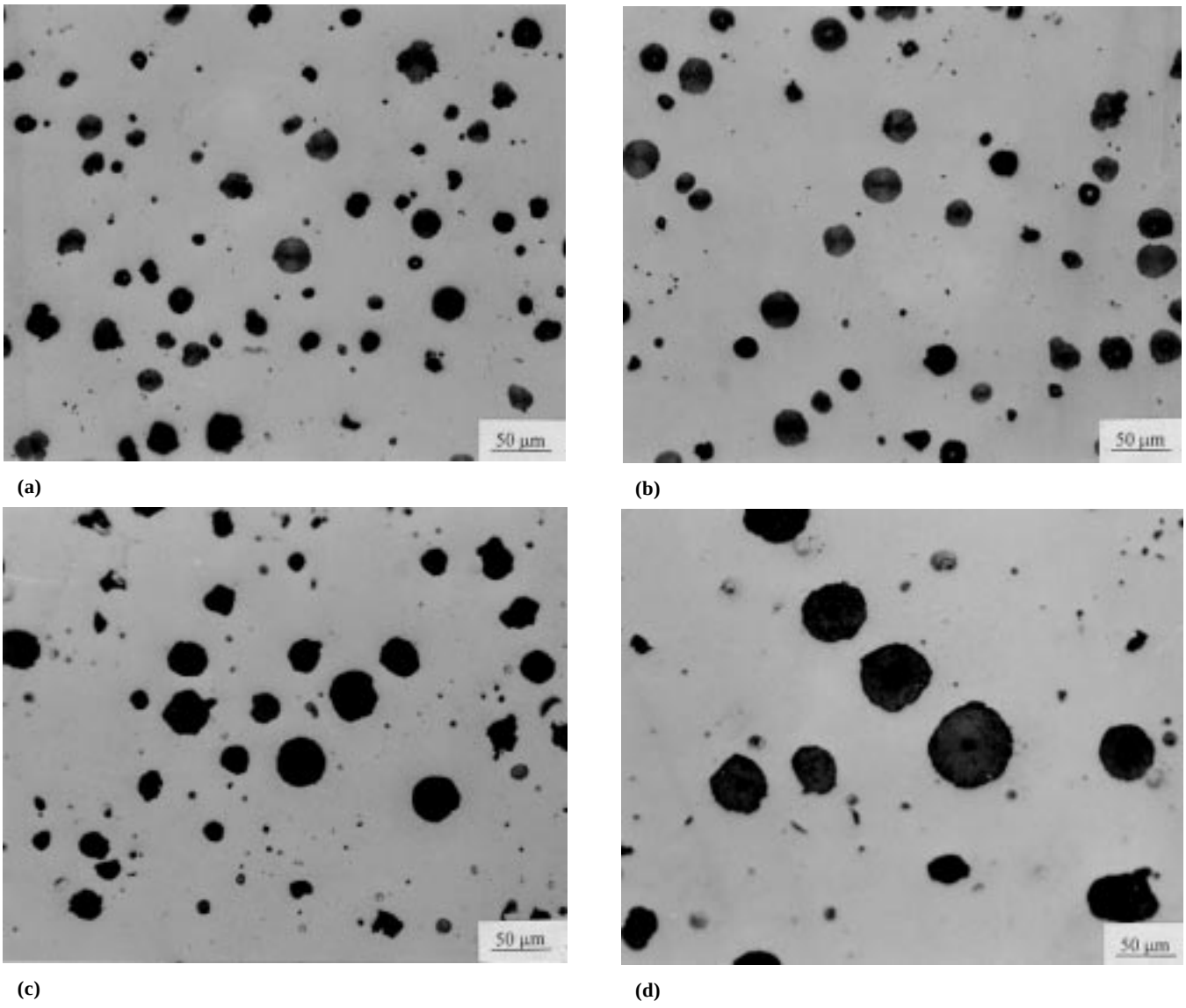

Fig. 2 Variation of nodule count with the cooling rate for heat 8. Cylinder diameter: C1, 15.5 mm; C2, 22.5 mm; C3, 30 mm; C4, 53.5 mm

3. Results

A typical microstructure observed in this study is shown in Fig. 1. This microstructure consisted of graphite nodules surrounded by a ferrite shell and pearlite. Figure 2 illustrates the variation of nodule count with the cooling rate for heat 8. It can be noted that the nodule count increased with increased cooling rates and that the nodule size increased as the cooling rate decreased. Figure 3 shows the nodule counts for all heats plotted as a function of the cylinder diameter. As expected, the nodule count, N_A, augmented with increased inoculation percentage and with decreased cylinder diameter. Linear fitting of the data from Fig. 3 is given in Table 2. As observed, for 0% inoculation the nodule count decreased by a rate of 3.39 nodules/mm of increased diameter, while for 0.64% inoculation this rate was of 7.92. It should be noticed that the latter rate is about twice as large as the former rate. This means that, for this experimental condition, the nodule count can be made approximately twofold by the inoculation treatment for a given mold diameter. These results can be generalized by taking into account that the geometric or casting modulus, M_c, for a cylinder is a quarter of its diameter.

Figure 4 shows the variation of pearlite percentage as a function of the cylinder diameter for each inoculation percentage. It can be observed that the amount of pearlite was reduced with decreased cooling rates and with increased inoculation percentages. Thus the lowest pearlite values were those located at the largest mold diameters and higher nodule count values.

Table 1 Chemical composition of the heats

Heat no.	Inoculation, %	Chemical element, %						
		C	S	Mn	Mg	Cu	Mo	Si
1	0	3.59	0.01	0.23	0.04	1.10	0.25	2.63
2	0.32	3.6	0.01	0.26	0.03	1.05	0.25	2.75
3	0.32	3.29	0.09	0.26	0.04	0.9	0.23	2.53
4	0.32	3.76	0.01	0.26	0.05	1.09	0.26	2.81
5	0.64	3.75	0.01	0.23	0.05	0.95	0.23	2.78
6	0.64	3.66	0.01	0.26	0.04	0.92	0.23	3.02
7	0.64	3.74	0.01	0.26	0.04	0.9	0.21	2.9

Table 2 Variation of nodule count as a function of the mold diameter or casting modulus

Inoculation, %	Linear equation of nodule count	
0	$N_A = 297 - 3.39 \cdot \text{diameter}$	$N_A = 297 - 13.56 \cdot M_c$
0.32	$N_A = 447 - 6.39 \cdot \text{diameter}$	$N_A = 447 - 25.56 \cdot M_c$
0.64	$N_A = 588 - 7.92 \cdot \text{diameter}$	$N_A = 588 - 31.68 \cdot M_c$

Table 3 Variation of pearlite percentage with the cylinder diameter

Inoculation, %	Linear equation of pearlite percentage
0	$90.52 - 0.35 \cdot \text{diameter}$
0.32	$92.86 - 0.40 \cdot \text{diameter}$
0.64	$92.83 - 0.68 \cdot \text{diameter}$

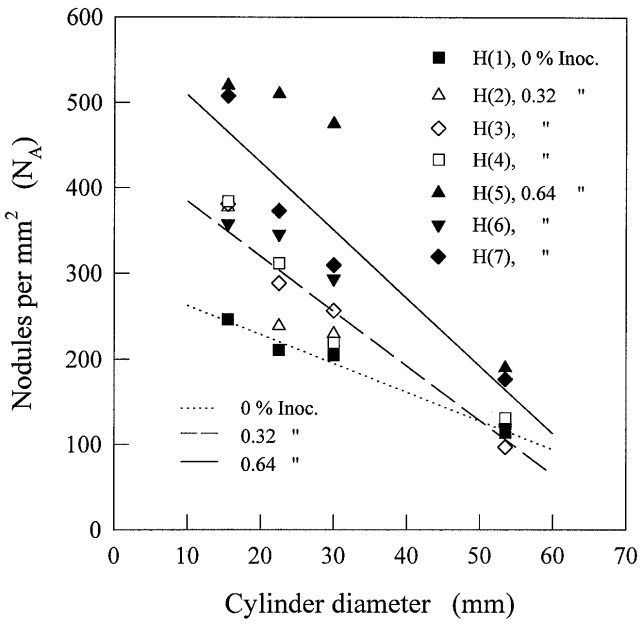

Fig. 3 Variation of nodule count as a function of cylinder diameter

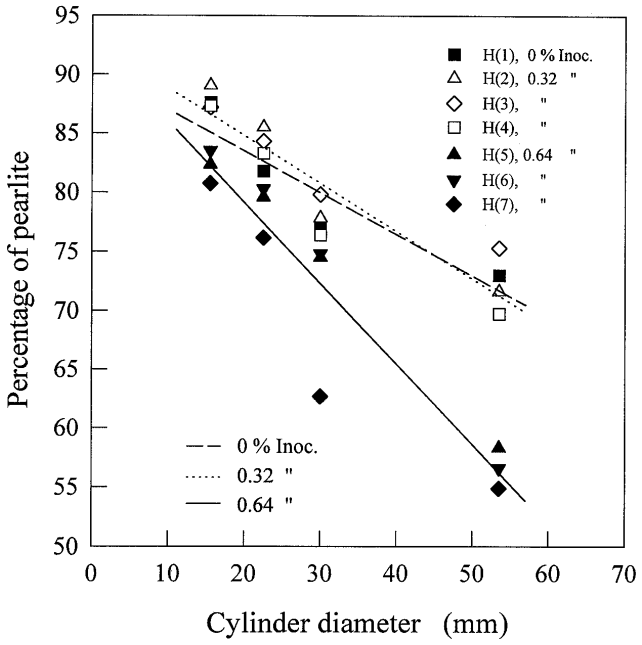

Fig. 4 Variation of percentage of pearlite as a function of the cylinder diameter and inoculation percentage

This is also shown by the coefficients of the linear regression of the data sets in Table 3. It was also observed that the 0.32% inoculation did not have a significant effect on the amount of pearlite, as its linear regression plotted very close to that of 0% inoculation.

Figure 5 presents the variation of pearlite percentage as a function of the nodule count for all heats. Data sets were grouped as a function of the cylinder diameter, and the corresponding linear regressions were obtained. It is worth noticing that at a given cooling rate (i.e. cylinder diameter), the pearlite percentage was reduced as the nodule count increased. It was also observed that the variation in the amount of pearlite is more sensitive at low nodule count. For instance, at low nodule count (cylinder 4), for which the nodule count varied approximately from 100 to 200, the pearlite content ranged from 55 to 80%. In contrast, at a higher nodule count, between 400 and 500 (cylinder 1), the percentage of pearlite varied only between 82 and 88%.

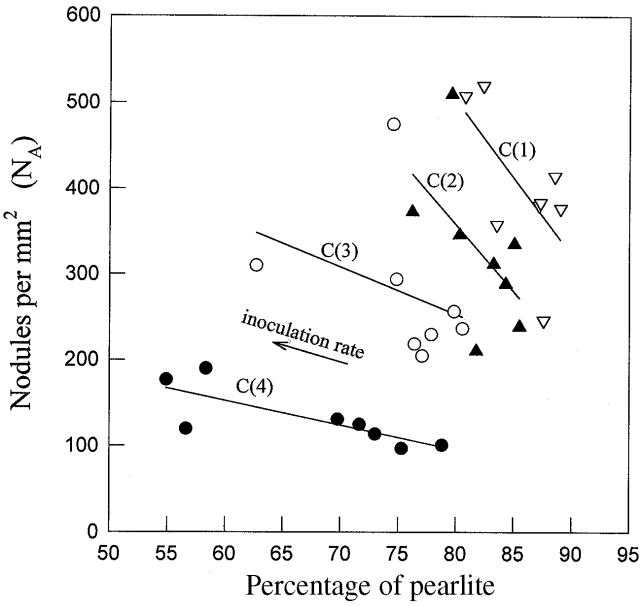

Fig. 5 Variation of nodule count as a function of the pearlite percentage for all cylinders: C1, 15.5 mm; C2, 22.5 mm; C3, 30 mm; C4, 53.5 mm

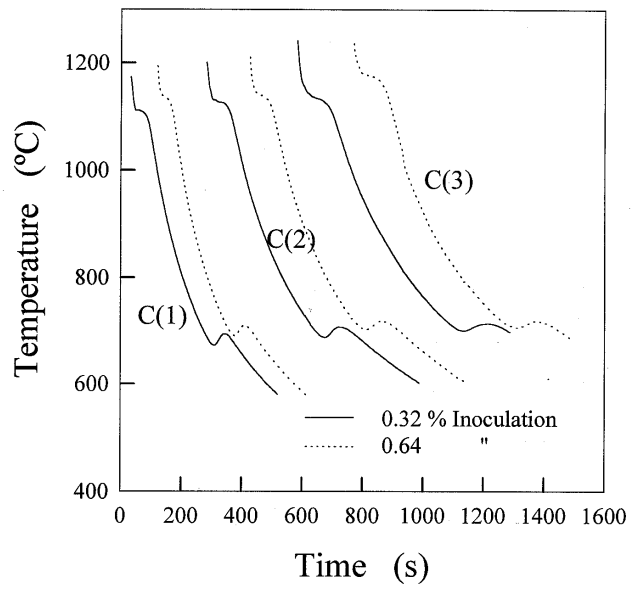

Fig. 6 Cooling curves for three cylinders of heats 4 and 5: C1, 15.5 mm; C2, 22.5 mm; C3, 30 mm

4. Discussion

The augmentation of the nodule count with increasing the cooling rate (Fig. 3) can be explained by considering the theory of the heterogeneous nucleation, which indicates that, for a given substrate, the nucleation is instantaneous when a specific undercooling is reached. Consideration of the same theory also indicates that the amount of nucleus increases with the undercooling. It is well known that large undercoolings are promoted by high cooling rates, which, for the present experimental conditions, were associated with the cylinders of small diameter. This is shown in Fig. 6, which displays cooling curves for three cylinders corresponding to heats 4 and 5 with 0.32 and 0.64% inoculation. Focus on the upper region of the figure (corresponding to the eutectic reaction), allowed observation that in each of the heats, the undercooling augmented as the cylinder diameter decreased. This is a result of the combination of the heat extraction ability of the system and the heat release associated with the solidification process.

The temperature arrest in the cooling curves is determined by thermal equilibrium between the amount of heat released and the amount of heat extracted by the system. It is noteworthy that the amount of heat released increases with the nodule count and the growing kinetics, which are enhanced, thus increasing the undercooling. Thus, increasing the heat extraction (for instance by reducing the cylinder diameter) means that the liquid metal needs larger undercooling before reaching the thermal equilibrium.

It is also interesting to observe in Fig. 6 that, for a given cooling rate, the magnitude of the undercooling was lower as the nodule count increased. The larger amounts of heat released, associated with higher nodule counts, shift the eutectic temperature arrest to higher values. A detailed picture of the solidification process of ductile iron can be found elsewhere (Ref 15, 16).

The products of the eutectoid transformation are the result of the competition process between the stable and metastable reactions. The eutectoid transformation, consisting in the decomposition of austenite, can occur either according to the stable mechanism ("ferritic reaction") to produce ferrite and graphite, or following the metastable mechanism in which ferrite and pearlite are formed ("pearlitic reaction") (Ref 10). Thus, if the eutectoid transformation occurs at a higher temperature than that for the metastable reaction, then nucleation and growth of ferrite are promoted and the pearlitic reaction is inhibited. In an analogous manner to the eutectic reaction, the temperature arrest is determined by the thermal equilibrium between the heat generated by the eutectoid transformation and the heat extraction capability through the mold—in other words, by the transformation kinetics and cooling rate.

The kinetics of the formation of ferrite depend on the number of available sites for nucleation and the growth kinetics. It is well known that the ferrite nucleates at the interface graphite/austenite; hence, increasing the nodule count can lead to an enhancement of the ferrite nucleation, yielding higher amounts of this phase in the microstructure matrix, as observed in Fig. 5 for each cooling rate. Furthermore, the growth of ferrite is controlled by the redistribution of the carbon rejected at the austenite/ferrite interface. As the cooling rate decreases, the time available for the carbon diffusion increases, resulting in higher amounts of ferrite in the matrix. As the carbon diffusion is a slow process, it is possible to achieve the temperature of metastable reaction (pearlite reaction temperature) during the cooling course. It is known that once the pearlite reaction is initiated, it proceeds with accelerated kinetics due to the short diffusion range associated to the cooperative growth of ferrite and cementite. Thus, high cooling rates promote the pearlite reaction, resulting in higher percentages of pearlite in the matrix structure as evidenced in Fig. 5 for cylinders 1 and 2, where in spite of the high nodule count, the pearlite promoting effect of the cooling rate is clear.

On the other hand, the eutectoid temperature arrest can be affected by the kinetics of the ferritic reaction. For instance, at a given cooling rate the enhancement of such kinetics (by increasing the nodule count) results in a higher temperature arrest. This is due to the exothermic effect associated to the formation of larger amounts of ferrite. For the present experimental conditions this effect is evidenced in the lower part of Fig. 6 by the lower undercooling observed for the curves containing higher nodule counts at a given cooling rate.

It is suggested that the onset temperatures for both reactions were very similar due to the fact that, for the studied cooling rates, a mix of pearlite and ferrite constituted the matrix. This results from the net effect of the different alloying elements. In considering the mean alloying elements present in the alloy, it is worth emphasis that some alloying elements act as ferrite promoters whereas others promote the pearlite reaction. It has been reported (Ref 7) that molybdenum and silicon, at the present levels, enhance the ferrite reaction by increasing the transformation temperature of austenite to ferrite. On the other hand, the combination of manganese and copper favor the pearlite reaction by increasing the temperature of pearlite formation (Ref 11-13) and depressing the temperature for ferrite formation.

5. Conclusions

Experimental work was carried out to study the effect of nodule count and cooling rate on the as-cast microstructure matrix of a Cu-Mo spheroidal graphite cast iron. The observed results allow for the following conclusions:

- The nodule count increased with increased inoculation percentage. Materials were more sensitive to this effect at high cooling rates. The variation of nodule counts with the cooling rate for each inoculation percentage was represented by a linear regression equation. The nodule count can be roughly duplicated by increasing the inoculation from 0 to 0.64% or by reducing the cylinder diameter from 53.5 to 15.5 mm.
- The amount of pearlite decreased as the cooling rate decreased, and this variation was more pronounced at low nodule count. Consideration of the net effect of the different parameters reveals that pearlite percentage varied from 55 to 90%. This variation was explained in terms of the combined effect of the kinetics of ferrite formation and the cooling rate.
- The relative amounts of ferrite and pearlite can be explained by the net effect of nodule count and cooling rate on the eutectoid arrest. This arrest was higher at low cooling rates, and for a given cooling rate, the temperature arrest also increased as the nodule count increased. The increasing of the temperature arrest promoted the ferrite formation. This was explained in terms of the combined effect of the kinetics of ferrite formation and the thermal phenomena involved.

References

1. B.V. Kovacs, On the Terminology and Structure of ADI, *AFS Trans.*, Vol 102, 1994, p 417-420
2. B.V. Kovacs, Heat Treating of Austempered Ductile Iron, *AFS Trans.*, Vol 99, 1991, p 281-286
3. K. Ogi, Y.C. Jin, and C.R. Loper, Jr., A Study of Some Aspects of the Austenitization Process of Spheroidal Graphite Cast Iron, *AFS Trans.*, Vol 96, 1988, p 75-82
4. T. Skaland and O. Grong, Nodule Distribution in Ductile Cast Iron, *AFS Trans.*, Vol 99, 1991, p 153-157
5. D.R. Askeland and S.S. Gupta, Effect of Nodule Count and Cooling Rate on the Matrix of Nodular Cast Iron, *AFS Trans.*, Vol 83, 1975, p 313-320
6. J.F. Wallace, P. Du, H.-Q. Su, R.J. Warrick, and L.R. Jenkins, The Influence of Foundry Variables on Nodule Count in Ductile Iron, *AFS Trans.*, Vol 103, 1995, p 812-822
7. D. Venugopalan, Prediction of Matrix Microstructure in Ductile Iron, *AFS Trans.*, Vol 98, 1990, p 465-469
8. E.N. Pan, W.S. Hsu, and C.R. Loper, Jr., Effects of Some Variables on the Matrix and Mechanical Properties of Ferritic Ductile Irons, *AFS Trans.*, Vol 96, 1988, p 645-660
9. S.K. Yu and C.R. Loper, Jr., The Effect of Molybdenum, Copper, and Nickel on the Pearlitic and Martensitic Hardenability of Ductile Cast Iron, *AFS Trans.*, Vol 96, 1988, p 8115-8118
10. W.C. Johnson and B.V. Kovacs, The Effect of Additives on the Eutectoid Transformation of Ductile Iron, *Metall. Trans. A*, Vol 94, 1978, p 219-229
11. J. Lacaze, C. Wilson, and C. Bak, Experimental Study of the Eutectoid Transformation in Spheroidal Graphite Cast Iron, *Scand. J. Metall.*, Vol 23, 1994, p 151-163
12. J. Lacaze, S. Ford, C. Wilson, and E. Dubu, Effects of Alloying Elements upon the Eutectoid Transformation in As-Cast Spheroidal Graphite Cast Iron, *Scand. J. Metall.*, Vol 22, 1993, p 303-309
13. J. Lacaze, A. Boudot, V. Gerval, D. Oquab, and H. Santos, The Role of Manganese and Copper in the Eutectoid Transformation of Spheroidal Graphite Cast Iron, *Metall. Trans. A*, Vol 28, 1997, p 2015-2020
14. M.J. Lalich and C.R. Loper, Jr., Effects of Pearlite-Promoting Elements on the Kinetics of the Eutectoid Transformation in Ductile Cast Irons, *AFS Trans.*, Vol 81, 1973, p 217-228
15. G. Lesoult, M. Castro, and J. Lacaze, Solidification of Spheroidal Graphite Cast Irons Part I: Physical Modelling, *Acta Mater.*, Vol 46 (No. 3), 1998, p 983-995
16. J. Lacaze, M. Castro, and G. Lesoult, Solidification of Spheroidal Graphite Cast Irons Part II: Numerical Simulation, *Acta Mater.*, Vol 46 (No. 3), 1998, p 997-1010